Electronic Supplementary Material (ESI) for Dalton Transactions

Supporting Information for:

Structure and Thermal Expansion in Tungsten Bronze $Pb_2KNb_5O_{15}$

Kun Lin,[1] Hui Wu,[2,3] Fangfang Wang,[1] Yangchun Rong,[1] Jun Chen,[1] Jinxia Deng,[1,4] Ranbo Yu,[1] Liang Fang,[5] Qingzhen Huang,[2] and Xianran Xing[1]*

[1]Department of Physical Chemistry, University of Science and Technology Beijing, Beijing 100083, China

[2]NIST Center for Neutron Research, National Institute of Standards and Technology, Gaithersburg, Maryland 20899-6102, United States

[3]Department of Materials Science and Engineering, University of Maryland,College Park, MD 20742-2115, United States

[4]Department of Chemistry, University of Science and Technology Beijing, Beijing 100083, China

[5]Key Laboratory of New Processing Technology for Nonferrous Metals and Materials, Ministry of Education, Guilin University of Technology, Guilin 541004, China

EXPERIMENT

Specific thermal capacity C_p measurements were carried out on a STA 449C thermal analyzer from RT to 800 °C. High temperature XRD (TTRIII, Rigaku, Japan, Cu $K\alpha$, λ = 1.5406 Å) data were collected from RT to 600 °C with a scanning rate of 4 ° / min for 2θ; The heating rate was 10 °C / min and the sample was hold for 15 min at a specified temperature to reach heat equilibrium.

The first-principles DFT calculations were performed using Vienna *ab initio* Simulation Package (VASP).[1-4] The electron-ion interaction was described using the projector augmented wave (PAW) method, the exchange correlation potential using the generalized gradient approximation (GGA) in the Perdew-Burke-Emzerhof (PBE) form. The cut-off energy for the basis set was 200 eV. Brillouin zone was sampled by 4 × 4 × 4 k-point mesh. In our present DFT calculations, a non-split model was used to simplify the calculation process, where the Pb^{2+} were put on the mirror plane instead of two splited sites in pentagonal sites (Figure S1b). A 1 × 1 × 2 supercell was built, where two K^+ and two Pb^{2+} ions are alternately distributed along [0 0 1] direction in one pentagonal site, shown in Figure S2.

RESULTS AND DISCUSSION

In the refining process, splits in pentagonal sites were included. Both Pb^{2+} and K^+ occupy 50% in pentagonal sites. Furthermore, the Pb^{2+} ($Pb_p(2)$, $Pb_p(3)$) itself also split on both sides of (0 2 0) mirror plane,[5] similar to $Pb_2KTa_5O_{15}$.[6] In PKN, there are two $Pb_p(2)$ or $Pb_p(3)$ and one $K_p(2)$ or $K_p(3)$ sites in one pentagonal space with

occupancy of 25% for Pb^{2+} and 50% for K^{+} (Figure S1a). To investigate the electron density distribution, DFT calculations were performed. Because of the complexity of the structure, a non-split model was used to simplify the calculation process, where the Pb^{2+} were put on the mirror instead of two splited sites in pentagonal sites (Figure S1b). A 1 × 1 × 2 supercell was built, where two K^{+} and two Pb^{2+} ions are alternately distributed along [0 0 1] direction in one pentagonal site, see Figure S5.

It should be noted that in DFT calculations, a simplified model was used because of calculation limit. We don't take into account the spilt of Pb in 15-coodination sites. The results can not be used to quantificationally determine the electronic structures. Not withstanding its limitation, this study does reveal the trend of charge distribution. A more reasonable model may be built in future studies

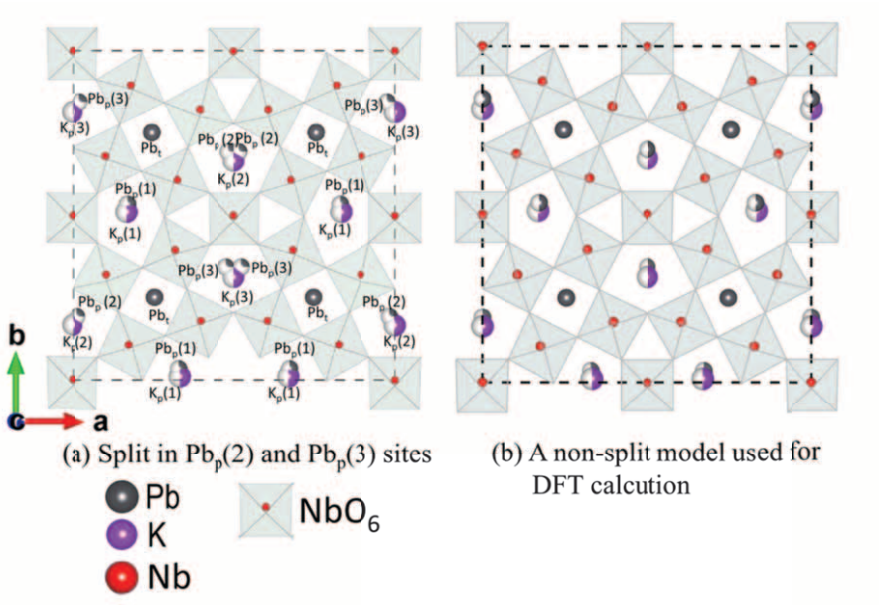

Figure S1. Our refined structure indicates that both Pb^{2+} and K^{+} occupy 50% in pentagonal sites. Furthermore, the Pb^{2+} ($Pb_p(2)$, $Pb_p(3)$) itself also split on both sides of (0 2 0) mirror. In PKN, there are two $Pb_p(2)$ or $Pb_p(3)$ and one $K_p(2)$ or $K_p(3)$ sites in one pentagonal sites with occupancy of 25% for Pb^{2+} and 50% for K^{+} (Table. S1). (a) shows split of Pb in pentagonal site ($Pb_p(2)$, $Pb_p(3)$) refined from netron powder diffraction at RT. (b) shows a non-split model used for DFT calculations. Percent of color on atoms present the protortion of occupancy. Compared to (a), in the non-split model, two $Pb_p(2)$ and $Pb_p(3)$ are put in the mirror instead of two splited sites. The occupancy of $Pb_p(2)$ and $Pb_p(3)$ in (a) is 0.25, and the value in (b) is 0.5. Sbuscript p means in pentagonal sites.

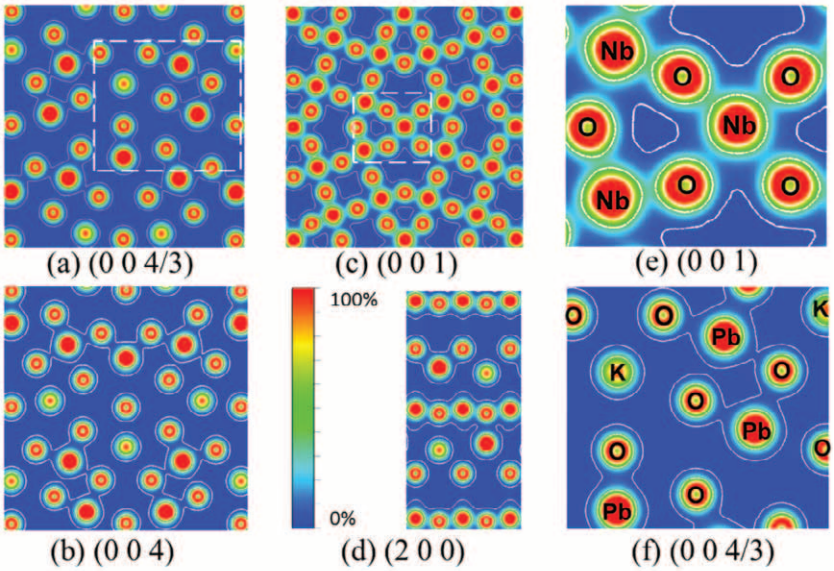

Figure S2. Electron density difference of PKN calculated by DFT in different planes (a) – (d); (e) and (f) are enlarged view of selected regions in (c) and (a), respectively. The 0 and 100% in color scale correspond to 0.2 and 3.5 $Å^{-3}$, contours from 0.2 to 1.7 $Å^{-3}$ by 1.5 $Å^{-3}$ step.

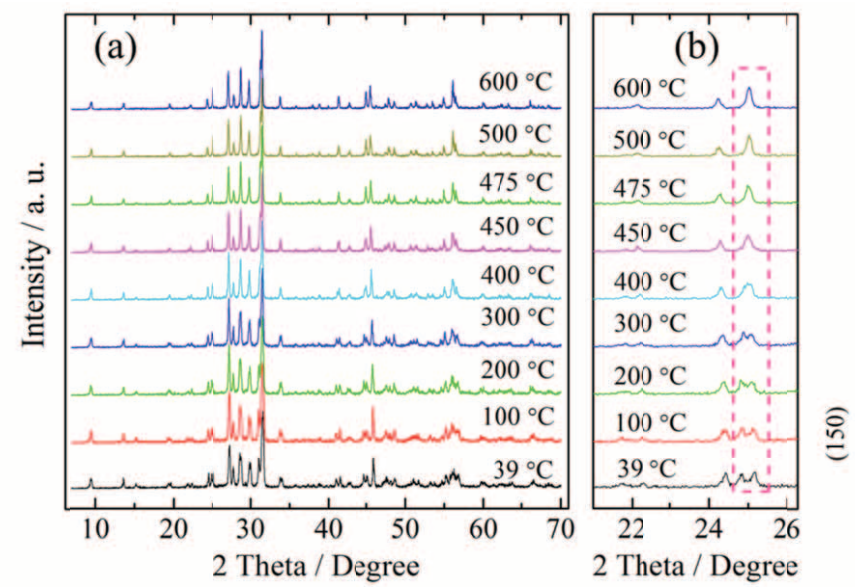

Figure S3. XRD patterns at different temperatures. (b) The evolution of (1 5 0) and (5 1 0) peaks.

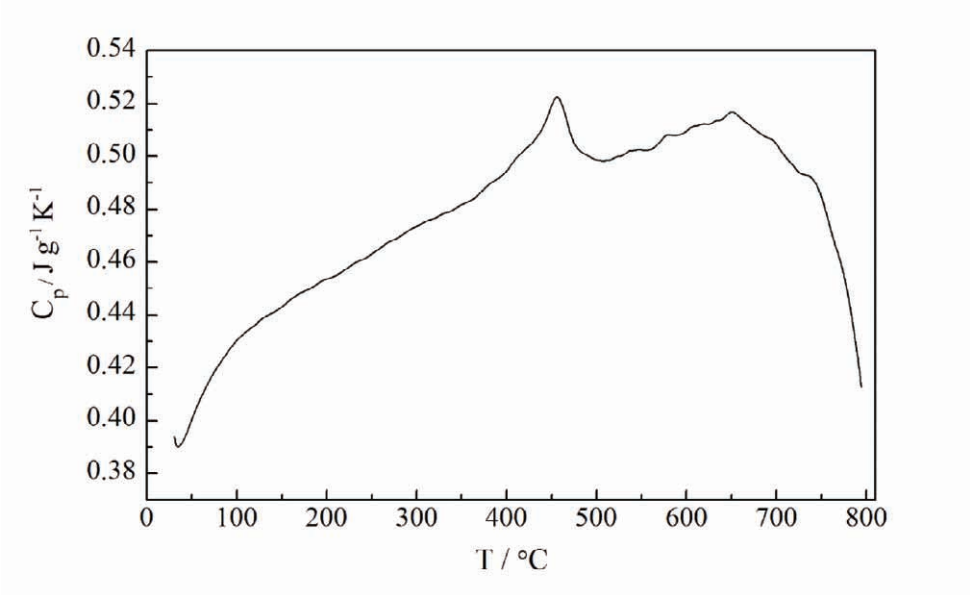

Figure S4. Temperature dependence of specific thermal capacity measured by DSC.

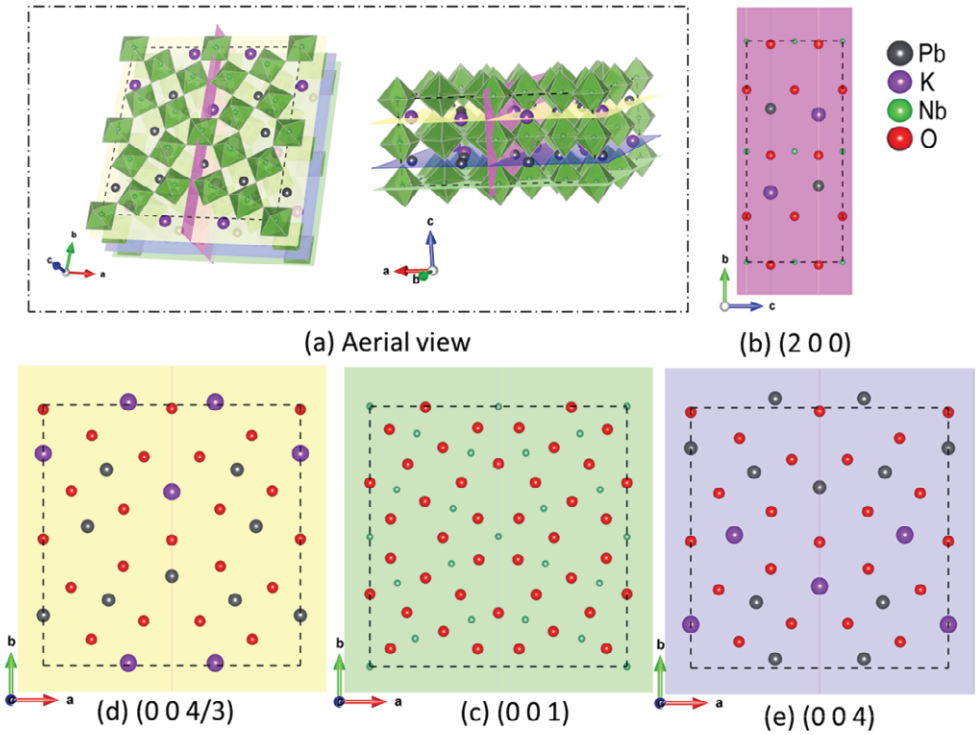

Figure S5. Different slices of the 1 × 1 × 2 supercell used for DFT calculations. (a), an aerial view of the model. The colored plane responds to slices in (b) – (e).

Table S1. Refined structural parameters of PKN at room temperature.

Atom	Sites	x	y	z	U_{iso}	Occ.
Nb(1)	2a	0.00000(0)	0.00000(0)	0.00000(0)	0.0175(9)	1.000(0)
Nb(2)	2a	0.00000(0)	0.49848(15)	0.00000(0)	0.0175(9)	1.000(0)
Nb(3)	4d	0.17615(4)	0.10766(11)	0.00000(0)	0.0073(4)	1.000(0)
Nb(4)	4d	0.31726(4)	0.39503(10)	0.00000(0)	0.0073(4)	1.000(0)
Nb(5)	4d	0.39546(5)	0.18023(10)	0.00000(0)	0.0073(4)	1.000(0)
Nb(6)	4d	0.10704(5)	0.32070(10)	0.00000(0)	0.0073(4)	1.000(0)
K_p(1)	4e	0.33106(17)	0.01059(18)	0.50000(0)	0.0262(31)	0.500(0)
K_p(2)	2b	0.00000(0)	0.16664(31)	0.50000(0)	0.0262(31)	0.500(0)
K_p(3)	2b	0.50000(0)	0.31335(34)	0.50000(0)	0.0262(31)	0.500(0)
Pb_p(1)	4e	0.32765(7)	0.03435(11)	0.50000(0)	0.0105(13)	0.500(0)
Pb_p(2)	4e	0.01658(12)	0.19331(14)	0.50000(0)	0.0105(13)	0.250(0)
Pb_p(3)	4e	0.52381(12)	0.34354(14)	0.50000(0)	0.0105(13)	0.250(0)
Pb_t	4e	0.25407(5)	0.25187(10)	0.50000(0)	0.0193(7)	1.000(0)
O(1)	2a	0.00000(0)	-0.01791(10)	0.50000(0)	0.0165(5)	1.000(0)
O(2)	2b	0.50000(0)	-0.01419(15)	0.50000(0)	0.0165(5)	1.000(0)
O(3)	4e	0.18697(7)	0.10043(11)	0.50000(0)	0.0165(5)	1.000(0)
O(4)	4e	0.31084(7)	0.38155(11)	0.50000(0)	0.0165(5)	1.000(0)
O(5)	4e	0.39045(6)	0.17083(11)	0.50000(0)	0.0165(5)	1.000(0)
O(6)	4e	0.10810(6)	0.30024(10)	0.50000(0)	0.0165(5)	1.000(0)
O(7)	4d	0.07968(6)	0.06945(11)	0.00000(0)	0.0172(4)	1.000(0)
O(8)	4d	0.14382(7)	0.20753(11)	0.00000(0)	0.0172(4)	1.000(0)
O(9)	4d	0.21619(3)	-0.00428(12)	0.00000(0)	0.0172(4)	1.000(0)
O(10)	4d	0.28640(7)	0.13483(10)	0.00000(0)	0.0172(4)	1.000(0)
O(11)	4d	0.41953(7)	0.06777(11)	0.00000(0)	0.0172(4)	1.000(0)

O(12)	2a	0.50000(0)	0.20618(13)	0.00000(0)	0.0172(4)	1.000(0)
O(13)	2a	0.00000(0)	0.27866(12)	0.00000(0)	0.0172(4)	1.000(0)
O(14)	4d	0.08053(6)	0.41688(12)	0.00000(0)	0.0172(4)	1.000(0)
O(15)	4d	0.21652(7)	0.34103(10)	0.00000(0)	0.0172(4)	1.000(0)
O(16)	4d	0.35270(6)	0.27652(11)	0.00000(0)	0.0172(4)	1.000(0)
O(17)	4d	0.42411(6)	0.41139(10)	0.00000(0)	0.0172(4)	1.000(0)

Subscript “p” means in 15-coordination site, “t” means in12-coordination site.

Table. S2. atomic patameters refined from NPD at 550 °C.

Name	Sites	x	y	z	U_{iso}	Occ.
Pb_p	8j	0.1411(10)	0.6871(8)	0.5000(0)	0.0434(35)	0.2500(0)
K_p	4h	0.1916(26)	0.6916(26)	0.5000(0)	0.1560(22)	0.5000(0)
Pb_s	2b	0.0000(0)	0.0000(0)	0.5000(0)	0.0430(13)	1.0000(0)
Nb1	2d	0.0000(0)	0.5000(0)	0.0000(0)	0.0213(12)	1.0000(0)
Nb2	8i	0.0736(3)	0.2150(3)	0.0000(0)	0.0222(6)	1.0000(0)
O1	2c	0.0000(0)	0.5000(0)	0.5000(0)	0.0391(21)	1.0000(0)
O2	8i	-0.0036(4)	0.3453(3)	0.0000(0)	0.0294(9)	1.0000(0)
O3	8j	0.0753(4)	0.2044(4)	0.5000(0)	0.0322(9)	1.0000(0)
O4	4g	0.2155(4)	0.2846(4)	0.0000(0)	0.0318(17)	1.0000(0)
O5	8i	0.1407(4)	0.0692(4)	0.0000(0)	0.0285(8)	1.0000(0)

Table. S3. Pb-O bond lengths in PbO_{15} (Pb_p-O) and PbO_{12} (Pb_t-O) polyhedral at RT. The shaded atoms are in the equatorial plane of PbO_{15} and PbO_{12} polyhedral (the same layer as Pb along c direction).

Atom 1	Atom 2	Count	d [Å]	Atom 1	Atom 2	Count	d [Å]
Pb_p3	O17	2 x	2.4901(19)	**Pb_p2**	O8	2 x	3.4718(21)
Pb_p2	O13		2.5103(22)	**Pb_p1**	O4		3.6972(25)
Pb_p2	O6		2.5243(30)	**Pb_p3**	O16	2 x	3.8175(22)
Pb_p3	O1		2.5351(32)	**Pb_p2**	O1		3.8218(32)
Pb_p1	O11	2 x	2.6229(13)	**Pb_p3**	O4		3.8505(26)
Pb_p1	O5		2.7037(27)	**Pb_p3**	O5		3.9162(31)
Pb_p1	O10	2 x	2.7691(19)	**Pb_p2**	O3		3.9902(26)
Pb_p1	O3		2.7722(21)	**Pb_p1**	O15	2 x	4.0772(24)
Pb_p1	O9	2 x	2.8743(13)	**Pb_p1**	O6		4.3752(28)
Pb_p3	O17	2 x	2.9135(20)	**Pb_t**	O4		2.5481(26)
Pb_p2	O6		2.9396(29)		O15	2 x	2.6224(17)
Pb_p2	O8	2 x	3.0057(20)		O16	2 x	2.6685(12)
Pb_p3	O4		3.0206(26)		O6		2.7396(18)
Pb_p2	O7	2 x	3.1775(25)		O5		2.8328(20)
Pb_p3	O16	2 x	3.1832(21)		O8	2 x	2.8864(14)
Pb_p3	O12	2 x	3.1880(29)		O10	2 x	2.9381(20)
Pb_p1	O2		3.1889(16)		O3		2.9814(25)
Pb_p1	O14	2 x	3.3171(21)				
Pb_p2	O7	2 x	3.4306(25)				
Pb_p2	O3		3.4637(27)				
Pb_p3	O5		3.4690(32)				

Table. S4. Pb-O bond lengths in PbO_{15} (Pb_p-O) and PbO_{12} (Pb_t-O) polyhedral at 550 °C. The shaded atoms are in the equatorial plane of PbO_{15} and PbO_{12} polyhedral (the same layer as Pb along c direction).

Atom 1	Atom 2	Count	d [Å]
Pb_p	O2	2 x	2.668 (9)
	O4	2 x	2.955(10)
	O1	1 x	2.967(11)
	O2(2)	2 x	3.057(7)
	O3	1 x	3.064(12)
	O5	2 x	3.081 (8)
	O3(2)	1 x	3.113(12)
	O3(3)	1 x	3.597(13)
	O5	2 x	3.711(11)
	O3(4)	1 x	3.8543(5)
Pb_t	O3	4 x	2.757 (4)
	O5	8 x	2.8031(28)

REFERENCES

1. Blöchl, P. E., *Phys. Rev. B* **1994,** *50*, 17953-17979.
2. Kresse, G., *Phys. Rev. B* **1996,** *54*, 11169-11186.
3. Kresse, G., *Phys. Rev. B* **1999,** *59*, 1758-1775.
4. Perdew, J. P.; Burke, K.; Ernzerhof, M., *Phys. Rev. Lett.* **1996,** *77*, 3865-3868.
5. Sciau, P.; Calvarin, G.; Ravez, J., *Acta Crystallogr. Sect. B: Struc. Sci.* **1999,** *55*, 459-466.
6. Sciau, P.; Lu, Z.; Calvarin, G.; Roisnel, T.; Ravez, J., *Materials Research Bulletin* **1993,** *28*, 1233-1239.